International Journal of Physical Sciences Vol. 4 (4), pp. 194-164,April, 2009
Available online at http://www.academicjournals.org/IJPS
ISSN 1992 - 1950 © 2009 Academic Journals

Full Length Research Paper

Adaptive lifting based image compression scheme for narrow band transmission system

Nishat Kanvel[1]* and Elwin Chandra Monie[2]

Thanthai Periyar Government Institute of Technology, Vellore-2, Tamilnadu, India.
Directorate of Technical Education, Chennai-25, Tamilnadu, India.

Accepted 8 April, 2009

To enable wireless internet and other data services using mobile appliances, there is a critical need to support content rich cellular data communication, including voice, text, image and video. However mobile communication of multimedia content has several bottlenecks including limited bandwidth of cellular networks, channel noise and battery constraints of the appliances. In this paper an efficient adaptive data codec for still images that can significantly minimize the energy required for wireless image communication in a narrowband system while meeting bandwidth constraints of wireless network, image quality and latency constrains of the wireless services is presented. Based on wavelet image compression an efficient wavelet Image compression algorithm (AEWICNBTS) for lossless compression of still images, enabling significant reduction in computation as well as communication energy needed with minimal degradation of image quality is proposed additionally, the wavelet image compression parameter that can be used to effect trade offs between the energy savings, quality of image and required communication bandwidth is identified. A dynamic configuration methodology that selects the optimal set of parameters to minimize energy under network service, appliance constrains is also presented.

Key words: Image compression, adaptive, lifting, narrow band, transmission system.

INTRODUCTION

One of the major challenges in enabling image transmitssion will be the need to process and transmit a very large volume of data through narrow band. While significant improvement in bandwidth is expected with future wireless access technologies, improvement in transmission technology lags the rapidly growing energy requirements of future wireless and wired data services. One approach to mitigate to this problem is to reduce the volume of multimedia data transmitted over the wireless and wired channel via data compression techniques.

This has motivated active research on multimedia data compression techniques such as JPEG (Antonini et al., 1996; Sweldens, 1995), JPEG 2000 (Daubechies and Sweldens, 1996) and MPEG.These approaches concentrate on achieving higher compression ratio without sacrificing the quality of the image. However these efforts ignore the energy consumption during compression and RF transmission.

*Corresponding author. E-mail: nishatkanvel@yahoo.com.

Since images will constitute a large part of future wireless data, it is necessary to focus on energy efficient and adaptive image compression and communication techniques. Therefore using wavelet image compression an energy efficient wavelet image transform technique is used to eliminate computation of certain high-pass coefficients of an image (Yin and Balchen, 1997).

Digital communication allows more flexibility to the applications at only a fraction of a cost. Certain class of network protocols (ISDN, GSM, and also ATM) allows bandwidth reservation [Russell 93] that enables a smooth service to the user of the application. ISDN and also the GSM phase 2 HSCSD circuit-switched connection provides a user-requested, fixed n _ 64 kbps (n _ 9:6 kbps for HSCSD) bandwidth. Multipoint connections could be realized over a specialized service provider, to which point-to-point connections of individual participants are to be made. A connection of fixed bandwidth is usually established before starting a session and due to severe variations in network traffic imposed by remote imaging services, a much higher bandwidth is to be allocated (and paid for) to a service that it would be statistically required.

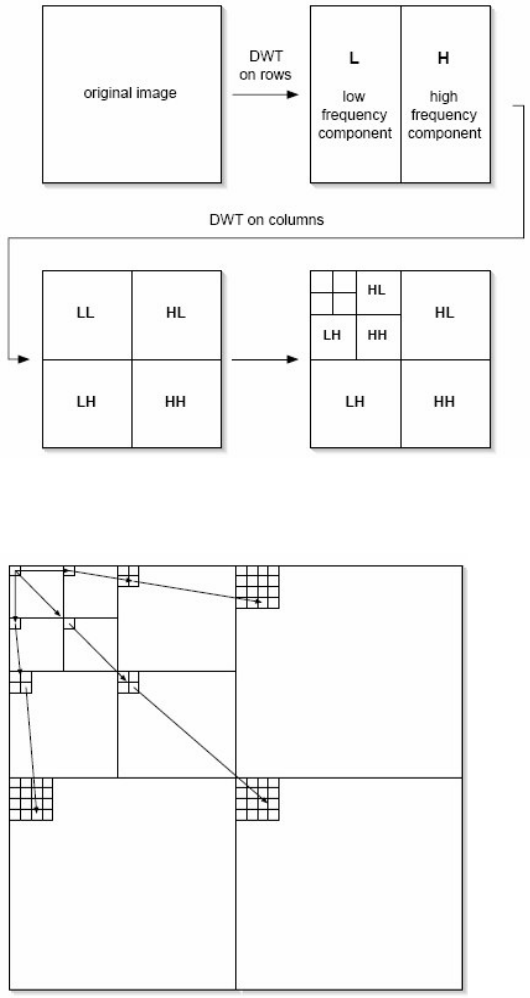

Figure 1. 2D wavelet decomposition.

On the other side, statistical multiplexing and bandwidth sharing (Ethernet, Internet) makes higher data throughput over a physical line but adds additional limitations in terms of uncontrolled queuing delays, buffer overflows etc. that may seriously degrade the overall quality of service.

In this paper an efficient adaptive data codec for still images that can significantly minimize the energy required for wireless image communication in a narrowband system, while meeting bandwidth constraints of wireless network, image quality and latency constrains of the wireless services is presented.

DISCRETE WAVELET TRANSFORMS (DWT)

For Wavelet transforms to be calculated using computers the data must be discretised. A continuous signal can be sampled so that a value is recorded after a discrete time the, sampling rate is uniform but with wavelets, the sampling rate can be changed when the scale changes. Higher scales will have a smaller sampling rate.

According to Nyquist Sampling theory, the new sampling rate N2 can be calculated from the original rate N1 using the following:

N = S1/S2 (N1)

where s1 and s2 are the scales. So every scale has a differrent sampling rate.

After sampling the Discrete Wavelet Series can be used, however this can still be very slow to compute. The reason is that the information calculated by the wavelet series is still highly redundant, which requires a large amount of computation time. To reduce computation a differrent strategy was discovered and Discrete Wavelet Transform (DWT) method was born as shown in Figure 1.

9/7 FLOAT TRANSFORM

Analysis of filter coefficient

$$\{h_{-4}, h_{-3}, h_{-2}, h_{-1}, h_0, h_1, h_2, h_3, h_4\}$$
$$\{g_{-3}, g_{-2}, g_{-1}, g_0, g_1, g_2, g_3\}$$

The 9/7 Float DWT uses two sets of analysis filter coefficients (.taps.) The numerical values of the two sets of taps are specified in Table 1.

Analysis of Filter Operations

For N > 1, let

$$\{x_0, x_1, x_2, \ldots, x_{2N-1}\}$$

denote a one-dimensional signal consisting of 2N samples. The one-dimensional float DWT
is defined by the following pair of analysis filter operations:

$$C_j = \sum_{n=-4}^{4} h_n x_{2j+n}; \qquad D_j = \sum_{n=-3}^{3} g_n x_{2j+1+n}; \quad j = 0,1,\ldots,N-1 \tag{3}$$

The outputs Cj, Dj are referred to as the coefficients of the wavelet transform. In equation 3 the filter taps are chosen so that Cj and Dj represent low-pass and high-pass outputs respectively.

That is, Cj is a smoothed (low-pass) version of the orignal signal while Dj contains high-pass information. At the beginning (left boundary) of the signal, equation 3 requires signal values with negative indices and at the end (right boundary) of the signal, it requires signal values with indices exceeding 2*N*-1.

9/7 INTEGER TRANSFORM

The present single-level, 1-d Integer DWT shall map a signal vector (equation 2) to two sets of wavelet

Table 1. Comparison table for 9/7 transform and 5/3 transform.

IMAGES	9/7 Transform				5/3 Transform			
	PSNR	CR	ENC Time	DEC Time	PSNR	CR	ENC Time	DEC Time
Cameraman	35.21	24.27	0.172	0.641	55.06	9.74	0.157	0.25
Rice	39.87	27.78	0.156	0.672	57.44	11.65	0.125	0.234
Rose	38.92	29.62	0.172	0.656	66.97	12.69	0.125	0.218
Hibiscus	42.04	27.51	0.156	0.734	56.25	11.10	0.109	0.219

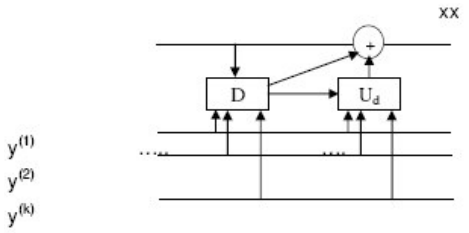

Figure 2. Adaptive update lifting scheme.

co-efficients, one high-pass set, Dj , and one low-pass set, Cj, in accordance with equations 5 and 6. Special boundary filters are required at either end of the signal, and lead to adapted formulas for j=0, j=N-2, and j=N-1.Equations 5 and 6 define the integer transform that shall be used with this Recommended Standard.

Given input values of xi, the *Dj* values in equation 5 shall be computed first and used subsequently to compute *Cj* values in equation 6.

$$
\begin{aligned}
D_0 &= x_1 - \left\lfloor \frac{9}{16}(x_0 + x_2) - \frac{1}{16}(x_2 + x_4) + \frac{1}{2} \right\rfloor \\
D_j &= x_{2j+1} - \left\lfloor \frac{9}{16}(x_{2j} + x_{2j+2}) - \frac{1}{16}(x_{2j-2} + x_{2j+4}) + \frac{1}{2} \right\rfloor \qquad for\ j = 1,\ldots,N-3 \\
D_{N-2} &= x_{2N-3} - \left\lfloor \frac{9}{16}(x_{2N-4} + x_{2N-2}) - \frac{1}{16}(x_{2N-6} + x_{2N-2}) + \frac{1}{2} \right\rfloor \\
D_{N-1} &= x_{2N-1} - \left\lfloor \frac{9}{8}x_{2N-2} - \frac{1}{8}x_{2N-4} + \frac{1}{2} \right\rfloor
\end{aligned}
\tag{5}
$$

$$
\begin{aligned}
C_0 &= x_0 - \left\lfloor -\frac{D_0}{2} + \frac{1}{2} \right\rfloor \\
C_j &= x_{2j} - \left\lfloor -\frac{D_{j-1} + D_j}{4} + \frac{1}{2} \right\rfloor \qquad for\ j = 1,\ldots,N-1
\end{aligned}
$$

GENERAL ADAPTIVE UPDATE LIFTING

We consider a (K + 1) band Filter bank decomposition with inputs x, y (1), y (2), y (3)….y (k), with k≥1, which represent the polyphase components of the analyzed signal. The first polyphase component, x, is updated using the neighboring signal elements from the other polyphase components, thus yielding an approximation signal. Subsequently, the signal elements in the polyphase components y (1), y (2)…y (K) are predicted using the neighboring signal elements from the approximated polyphase component and the other polyphase components. The prediction steps, which are non-adaptive, result in detail coefficients. The adaptive update step is illustrated in Figure 2. Here, x and y (1), y (2)…y (K) are the input for a decision map D, whose output at location n is binary decision d_n = D {y (1), y (2)…y (K)} ∈ {0,1}.

Combining norms technique

The input images x, y1, y2 and y3 are obtained by a polyphase decomposition of an original image x0 is given by,

$$x\,(m, n) = x0(2m, 2n)$$

In this decomposition, xx is called the approximation band and y1', y2', y3' are called the horizontal, the vertical and the diagonal detail bands respectively. At every position n = (m, n), the update step is triggered by the outcome

$$d_n = D(x, y_1, y_2, y_3)(n)$$

Where D represents the decision map. The output d_n triggers the specific choice of the update step in the following sense (Figure 3).

$$xx(n) = \alpha_{dn} x(n) + \sum_{j=1}^{3} \mu_{dn,j}\, y_j(n)$$

Where α_{dn} and μ_{dn} are the filter co-efficient. Note that the filter coefficients depend on the decision d_n which may change depending on the local characteristics of the input signals. We assume that the decision map only depends of the gradient vector v (n), with components $v_j(n)$ given by;

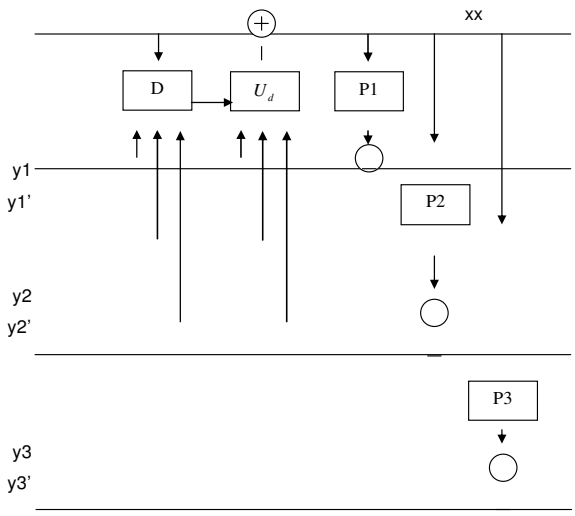

Figure 3. 2D wavelet decomposition comprising an adaptive update lifting step (left) and three consecutive prediction lifting steps (right).

$$v_j(n) = x(n) - y_j(n), \quad j = 1,2,3.$$

The filter co-efficient in (1), assumed that

$$\alpha_d + \sum_{j=1}^{3} \mu_{d,j} = 1 \quad \text{For d = 0, 1, N -1,}$$

With $\alpha_d \neq 0$ for all d.

In this way, we present the way of constructing the decision map by comparing different norms, each of them capturing different orientation features. Let us consider N norms, denoted by $P_0, P_1, ..., P_{N-1}$, and a decision map which can take N values, $d(v) \in \{0,1,...., N-1\}$. The decision criterion will be based on the comparison, at each sample, between the values of the norms. In this project considering N = 3, a possible construction of the decision maps, and hence of the decision regions, and its corresponding filter equations are described on the relations below.

Decision Region I

$$d = 1 \Leftrightarrow \begin{cases} P_1(v) < P_3(v) \\ P_1(v) \leq P_2(v) \end{cases} \Rightarrow \text{xx = 0.4 * y + (0.2*yh+0.2*yv+0.2*}$$

Decision Region II

$$d = 2 \Leftarrow \begin{cases} P_2(v) < P_3(v) \\ P_3(v) < P_1(v) \end{cases} \Rightarrow \text{xx = 0.5 * y + (0.2)*(yh)+(0.15)*yv+(0.15)*yd}$$

Decision Region III

$$d = 3 \Leftarrow \begin{cases} P_3(v) \leq P_1(v) \\ P_3(v) \leq P_2(v) \end{cases} \Rightarrow \text{xx = 0.45 * y + (0.2)*(yh)+(0.2)*yv+(0.15)*y}$$

NORMS

Let v (n) be the gradient vector with components, $(v_1(n), v_2(n), ...v_N(n)))^T$ (where T represents transposition), then

L_1 norm is defined as,

$$P_1(v) = \sum_{j=1}^{N} |v_j|$$

L_2 norm is defined as,

$$P_2(v) = (\sum_{j=1}^{N} v_j{}^2)^{\frac{1}{2}}$$

In general, the 'r'th norm is defined as,

$$P_r(v) = (\sum_{j=1}^{N} v_j{}^r)^{\frac{1}{r}}$$

And the L^∞ norm is defined as, $P_\infty(v) = \max|v_j|$, $j = 1,2,....N.$

The gradient vector at synthesis side is given by v' (n) with components $v'_j(n) = xx(n) - y'_j(n)$, $j = 1,2,....J.$ is related to gradient vector at analysis side v (n) by means of the linear relation $v'(n) = A_d v(n)$, Where $A_d = I - ub_d^T$, I is the $J \times J$ identity matrix, and $u = (1,....,1)^T$, $b_d = (\mu_{d,1}, ..., \mu_{d,J})^T$ are vector of length J. The super index 'T' denotes transposition. To have Perfect Reconstruction (PR), we must be able to recover the decision D_n from the gradient vector at synthesis $v'(n) = A_d v(n)$. That is, for all n,

$$D'(x', y_1', y_2', y_3')(n) = D(x, y_1, y_2, y_3)(n)$$

Similar to analysis, here also constructed the decision Map, and hence of the decision regions, and its corresponding filter equations are described on the relations below, as well as the necessary and sufficient condition for

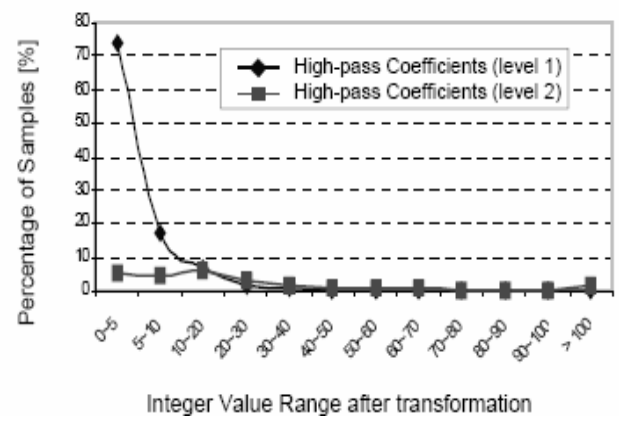

Graph 1. Computation and communication of high-pass coefficients

Perfect Reconstruction (PR) specified.

ENTROPY ENCODING AND DECODING

Entropy encoding

The encoding process is the main source of actual compression. Entropy encoding is used to reduce the redundancy of bits (pixel values) of images. Huffman coding and run Length coding is combined to give a better compression.

EFFICIENT WAVELET IMAGE COMPRESSION ALGORITHM (EWICA)

Analysis of Energy Consumption

To determine the energy efficiency of each algorithm, we use a metric that is independent of the detailed implementation of the algorithm. We analyze energy efficiency by determining the number of times certain basic operations are performed for a given input, which in turn determines the amount of switching activity, and hence the energy consumption. For example, in the forward wavelet decomposition using the above filter, 8 shift and 8 add operations are required to convert the sample image pixel into a low-pass coefficient. Similarly, high-pass decomposition requires 2 shift and 4 adds.

We model the energy consumption of the low/high-pass decomposition by counting the number of operations and denote this as the computational load.

Computational load:

$$C_{AWIC} = MN(12A+10S)\sum_{i=1}^{L}\frac{1}{4^{i-1}} = MN(12A+10S)\frac{1-4^{-L}}{1-4^{-1}} \le \frac{4}{3}MN(12A+10S)$$

Data- access load:

$$C_{READ\_AWIC} = C_{WRITE\_AWIC} = 2MN\sum_{i=1}^{L}\frac{1}{4^{i-1}} \le \frac{8}{3}MN$$

The overall computation energy is computed as a weighted sum of the computational load and data-access load. From our implementation experiments, we found that the add operation requires two times more energy consumption than the shift operation, and the energy cost of the data-access load is 2.7 times more than the computational load.

We also estimate the communication energy by C*R, where C is the size of the compressed image (in bits) and R is the per bit transmission energy consumed by the RF transmitter. Having analyzed the sources and magnitude of energy consumption in the wavelet transform, we next present techniques to minimize the computation energy as well as communication energy needed in wavelet-based image compression and wireless transmission.

Algorithm (EWICA)

EWICA exploits the numerical distribution of the high-pass coefficients to judiciously eliminate a large number of samples from consideration in the image compression process. The figure below illustrates the distribution of high-pass coefficients after applying a 2 level wavelet transform to the 512 .*512 Lena image sample. We observe that the high-pass coefficients are generally representted by small integer values. For example, 80 % of the high-pass coefficients for level 1 are less than 5. Because of the numerical distribution of the high-pass coefficients and the effect of the quantization step on small valued coefficients, we can estimate the high-pass coefficients to be zeros (and hence avoid computing them) and incur minimal image quality loss. This approach has two main advantages. First, because the high-pass coefficients do not have to be computed, EWICA helps to reduce the computation energy consumed during the wavelet image compression process by reducing the number of executed operations. Second, because the encoder and decoder are aware of the estimation technique, no information needs to be transmitted across the wireless channel, thereby reducing the communication energy re-quired.

Two techniques attempting to conserve energy by avoiding the computation and communication of high-pass coefficients (Graph 1). The first technique attempts to conserve energy by eliminating the least significant subband. Among the four subbands, we find that the diagonal sub-band (HHi) is least significant, making it the best candi-date for elimination during the wavelet transform step. We call this technique “HH elimination”. In the second scheme, only the most significant subband (low-resolu-tion information, LLi) is kept and all high-pass subbands (LHi, HLi, and HHi) are removed. We call this

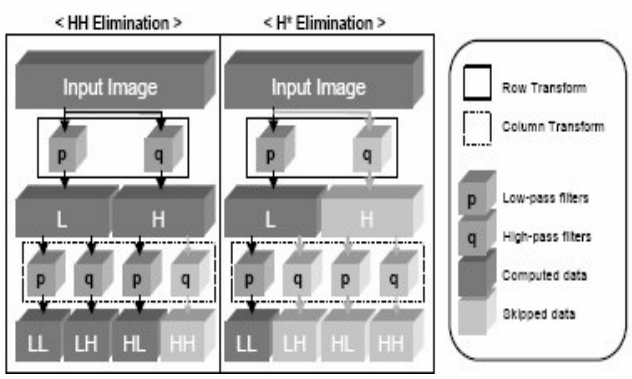

Figure 4. Data flow of the wavelet transform step with HH/H*

"H* elimination", because all high-pass subbands are eliminated in the transform step. We next present details of the HH and H* elimination techniques, and compare the energy efficiency of these techniques with the original AWIC algorithm which refers to the wavelet transform algorithm without elimination as described above.

Efficiency of elimination techniques

To implement the HH and H* elimination techniques (EWICA), we modified the wavelet transform step as shown in Figure 4. As explained in Section II-B, during the wavelet transform, each input image goes through the row and column transform decomposing the image into four subbands (LL, LH, HL and HH). However, to implement the HH elimination technique, after the row transform, the high-pass coefficients are only fed into the low-pass filter, and not the high-pass filter in the following co--lumn transform step (denoted by the lightly shaded areas as shown in Figure 4 under <HH Elimination>). This avoids the generation of a diagonal subband (HH).

To implement the H* elimination technique, the input image is processed through only the low-pass filter during both the row and column transform steps (shown by the lightly shaded areas under <H* Elimination>). We can therefore remove all high-pass decomposition steps during the transform by using the H* elimination technique.

We assume the elimination techniques are applied to the first E transform levels out of the L total transform levels. This is because the advantage of eliminating high-pass coefficients is more significant at lower transform levels. In the HH elimination technique, the computation load during the row transform is the same as with the AWIC algorithm. However, during the column transform of the high-pass subband resulting from the previous row transform, the high-pass subband (HH) is not computed. The results in Section II-C show that this leads to a savings of 1/4 MN (4A+2S) operation units of computational load (7.4 % compared to the AWIC algorithm).

Therefore, computational load when using HH elimination is represented as:

Computational load:

$$C_{HH} = \frac{MN(22A+19S)}{2}\sum_{l=1}^{E}\frac{1}{4^{l-1}} + MN(12A+10S)\sum_{l=E+1}^{L}\frac{1}{4^{l-1}}$$

Because the high-pass subband resulting from the row transform is still required to compute the HL subband during the column transform, we cannot save on "read" acesses using the HH elimination technique. However, we can save on a quarter of "write" operations (12.5 % savings) during the column transform since the results of HH subband are pre-assigned to zeros before the transform is computed. Thus, the total data-access load is given by:

Data-access load:

$$C_{READ\_HH} = C_{READ\_AWIC}, \quad C_{WRITE\_HH} = \frac{7}{4}MN\sum_{l=1}^{E}\frac{1}{4^{l-1}} + 2MN\sum_{l=E+1}^{L}\frac{1}{4^{l-1}}$$

NARROW BAND TRANSMISSION SYSTEM

Network specifications and connection management

Professional remote imaging applications of the past relied mostly on analogue technology over fixed cable connections, or when required, leased terrestrial and satellite links. The level of services in this case was limited to audio and video broadcast in PAL/NTSC quality. Such solutions are costly and the service management is hardly viable, especially when interactive co-operation of multiple participants is required. Digital communications allow more flexibility to the applications at only a fraction of a cost. Certain class of network protocols (ISDN, GSM and also ATM) allows bandwidth reservation [Russell, 93] that enables a smooth service to the user of the application. ISDN, and also the GSM Phase 2 HSCSD circuit-switched connection provides a user-re-quested, fixed n_64 kbps (n_9:6 kbps for HSCSD) band-width. Multi-point connections could be realized over a specialized service provider, to which point-to-point connections of individual participants are to be made.

A connection of fixed bandwidth is usually established before starting a session, and due to severe variations in network traffic, imposed by remote imaging services, a much higher bandwidth is to be allocated (and paid for) to a service that it would be statistically required. On the other side, statistical multiplexing and bandwidth sharing (Ethernet, Internet) makes higher data throughput over a physical line but adds additional limitations in terms of uncontrolled queuing delays, buffer overflows etc. that may seriously degrade the overall quality of service. Such approach is known as a packet-switched network approach. It has been widely accepted for non-real time data transfer. The traffic variance of voice, image and data traffic makes this approach hard for real-time applications;

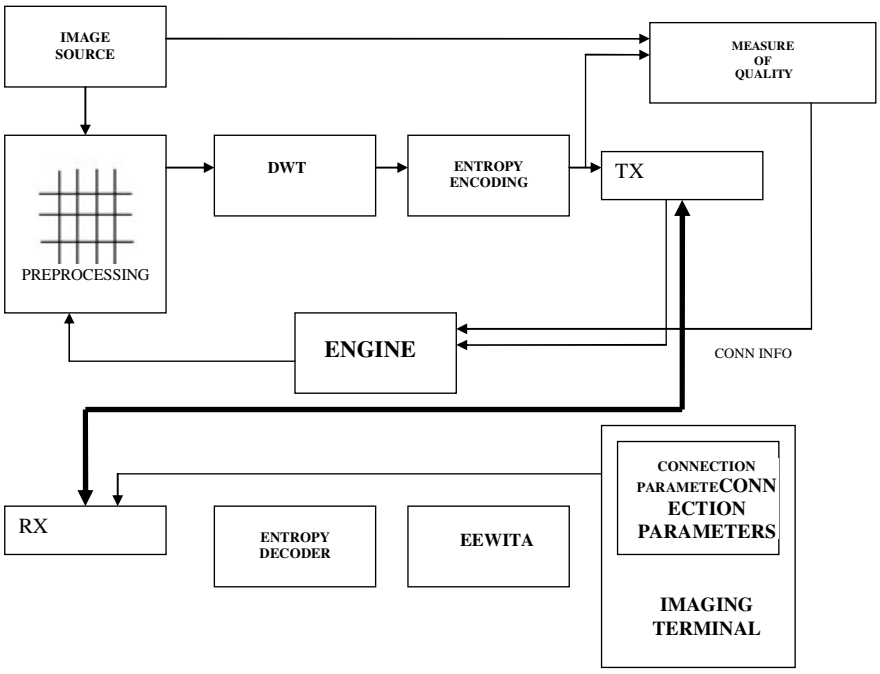

Figure 5. Optimised DWT network image transfer.

however bandwidth exploitation may be much higher (Venkatesh et al., 1998).

The ideal solution would be to let the service itself to control network behaviour and to maintain the underlying traffic throughput according to the type of the corresponding data source. According to the literature, a new active network structure of the future is proposed, that combines the above mentioned approaches into a so called smart–packet data transport (Decina). The future of teleworking, image-supported applications is definitively in the new arising integrated teleinformation systems that integrate user terminals, applications, service and data providers with the access and backbone network in-frastructure (Bergen, 1987).

The step towards such systems leads over the network-aware user applications that may efficiently exploit, allocate, or even control the network resources. An efficient remote imaging application should therefore not only handle data requests but also maintain good compression rate. To provide an optimal level of service, the application itself has to monitor network behaviour and to adapt the level of services to the momentarily available network resources (Figure 5). No matter what communication media, protocol or traffic routing we select, the dynamic of bandwidth allocation is a crucial part of an optimal application, or service [Jayant93]. Of a particular interest is a class of applications that allow at least partial user mobility. Wireless communications remain the area where specific care about network bandwidth and responsiveness should be taken care of; the resources are more limited and the cost per bit transferred is higher. A specific user may be given access to a public network, local private network or even a wired connection, and the application itself should maintain the present resources in the best possible way in terms of cost and availability.

EXPERIMENTAL RESULTS AND DISCUSSIONS

The adaptive and new efficient wavelet image compression is applied to some of the standard test images. The compression is performed using the MATLAB. The images are subjected to different levels of variations of the parameters namely transform level (TL), quantization level (QL) and elimination level during the process of compression. The simulation results obtained shows the compression of the images with their corresponding image quality.

The images from the database selected include the natural images cameraman. The tables representing the computation time, compression ratio and peak signal to noise ratio varying the different parameters are presented for various images taken as the test image. The Figure 6 represents the input image (camera man) used as a test image and Figure 7 shows the 9/7 reconstructed image. Figure 8 shows the validation for 9/7 reconstructed image which indicates the decoding time, encoding time PSNR and Compression ratio for the test image. For the same input image (as in Figure 6) the Figure 9 shows the 5/3 reconstructed image and Figure 10 shows the validation for 5/3 reconstructed image. Another test image used is the Rice image. Figure 11 shows the original rice image and the 9/7 Reconstructed rice image. Figure 12 shows the original rice image and the 5/3 Reconstructed rice image.

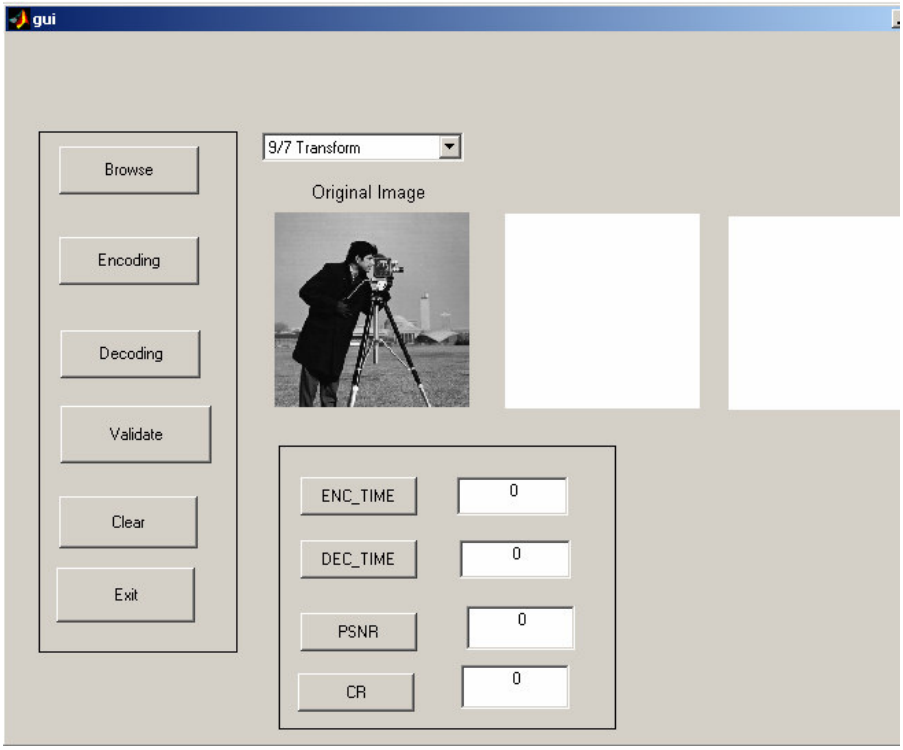

Figure 6. Input image.

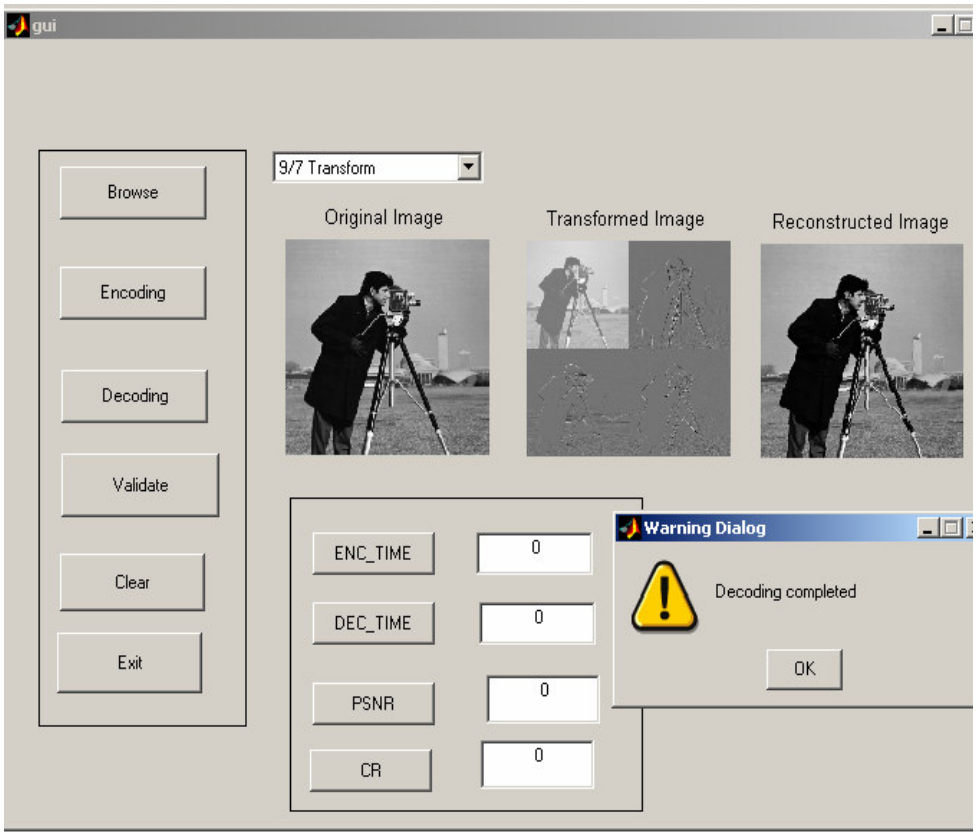

Figure 7. 9/7 Reconstructed image.

VALIDATION

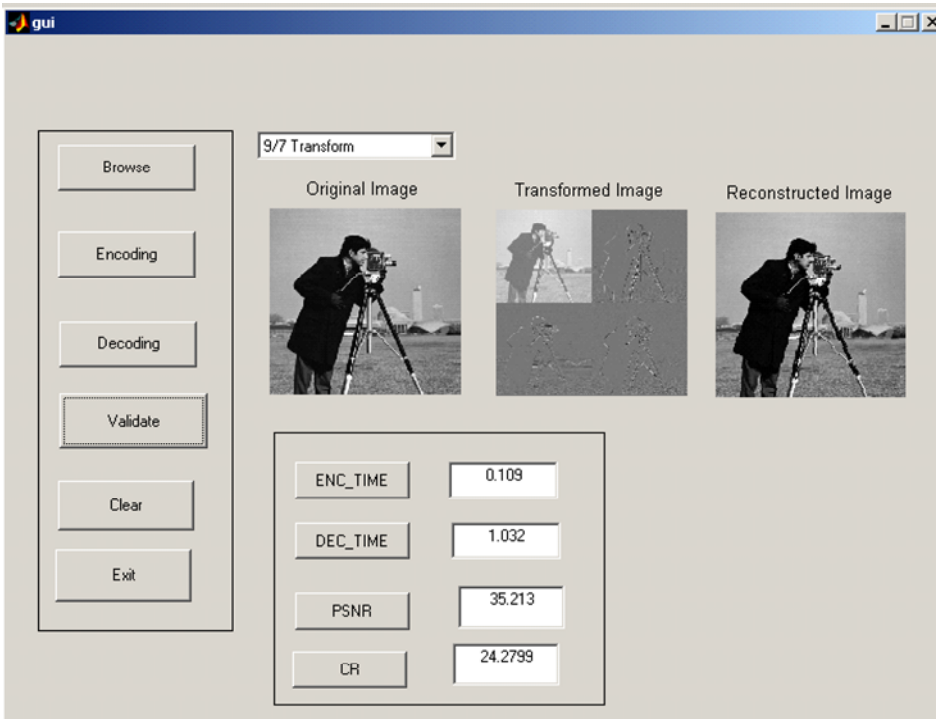

Figure 8. Validation of 9/7 Reconstructed Image.

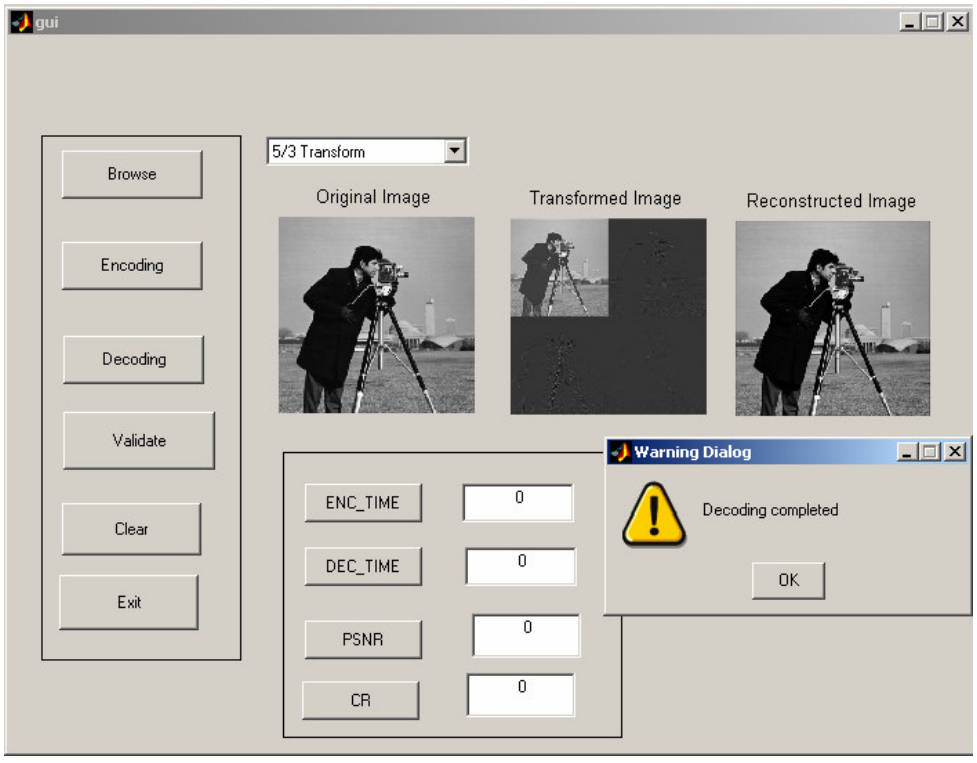

Figure 9. 5/3 Reconstructed Image.

VALIDATION

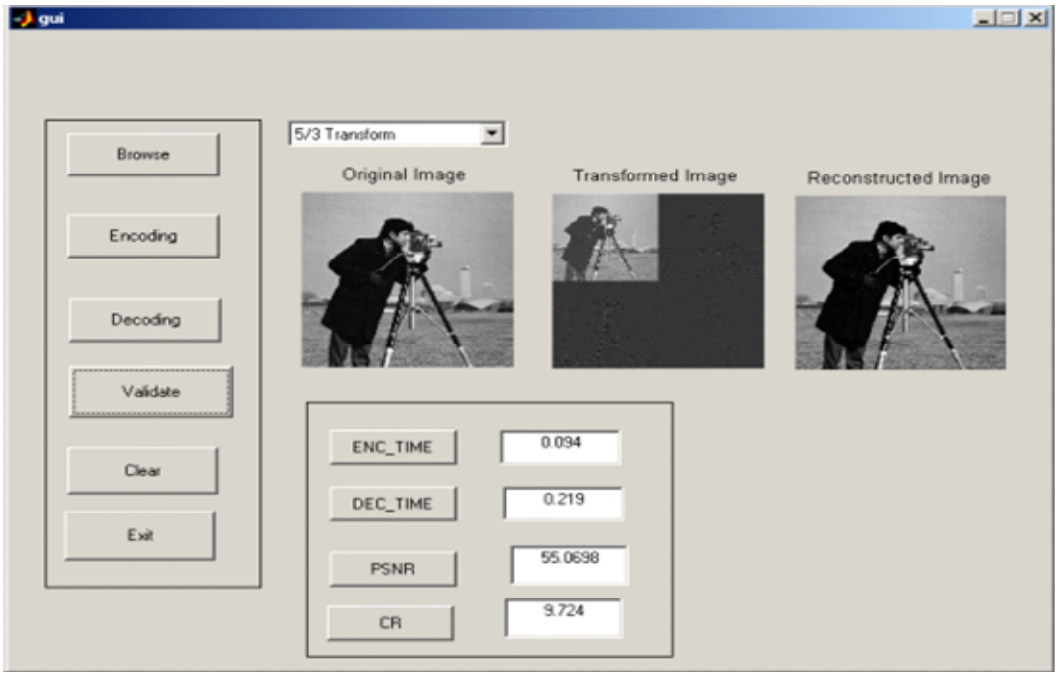

Figure 10. Validation of 5/3 Reconstructed Image.

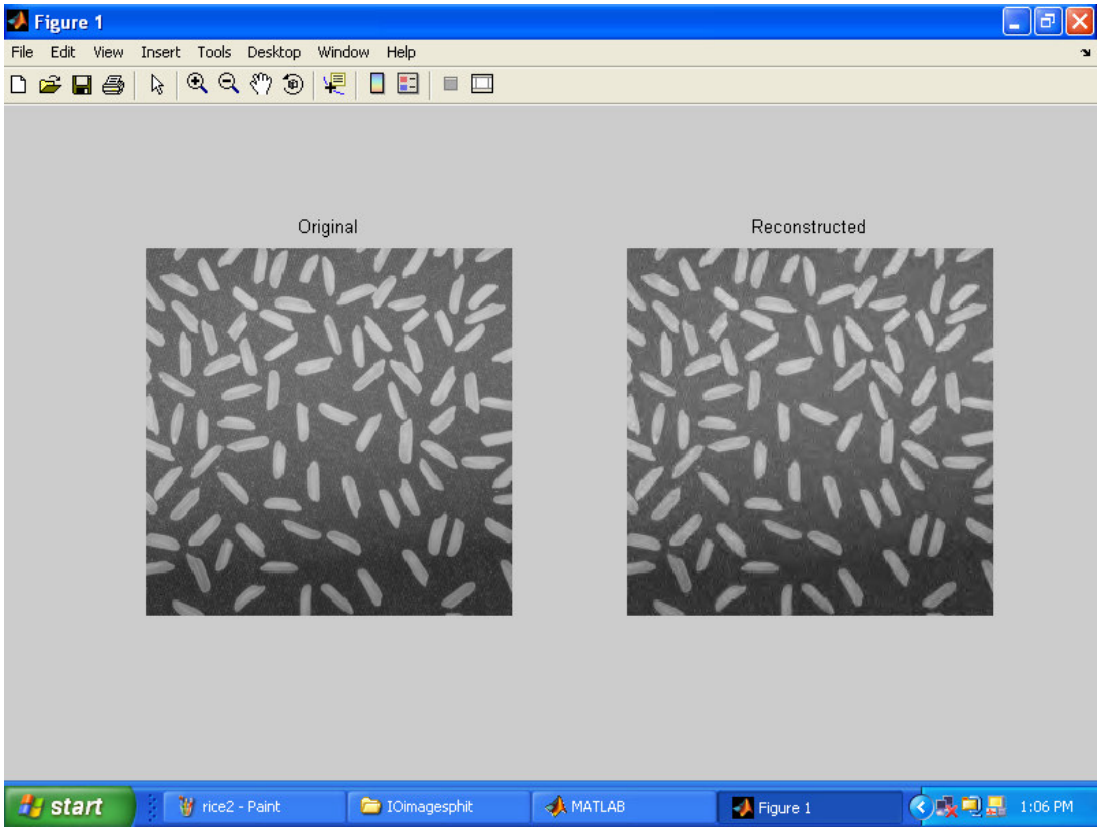

Figure 11. 9/7 reconstructed image.

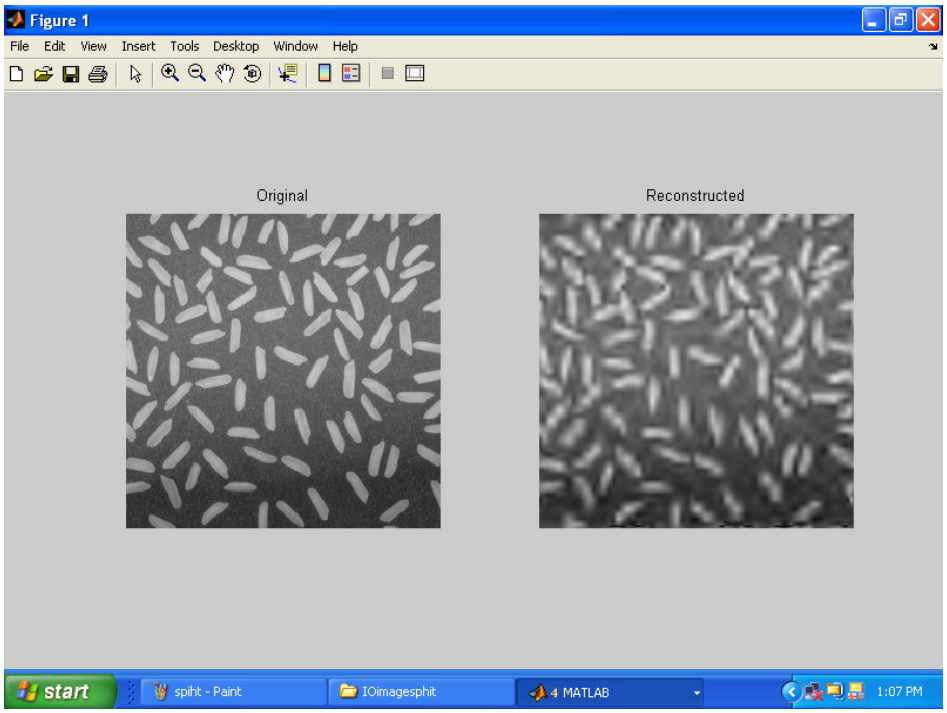

Figure 12. 5/3 reconstructed image.
+-*

Table 2. Compression results for 512x512 barbara image.

Bit rate(bpp)	Compression Ratio (:1)	PSNR(dB)		
		CZQ-WV	CZQ-WP	New method (AEWICNBTS)
1.0	7.8	34.14	36.45	36.75
0.8	10.2	32.10	34.15	35.10
0.6	14.50	32.00	32.86	33.45
0.4	21.00	28.10	29.95	30.42
0.2	41.00	25.45	27.46	30.01
0.1	81.20	24.25	23.12	25.25

OBJECTIVE RESULTS

PSNR and RMSE (root mean square error) offer a more objective way to compare various algorithms' performance with formulae for these metrics. Bit rates and PSNR values have been provided in Tables 1 and 2 the rate distortion curve for the Lena image is shown these are nominal values for bit rates of the various codecs that illustrate what might constitute typical operation in a desktop computing environment.

REFERENCES

Antonini M, Barlaud M, Mathieu P, Daubechies I (1996). Image coding using wavelet transform. IEEE Trans. Image Process. 1(2): 205-219.
Bergen (1987). Method for transmitting a high resolution image over a narrow band communication channel. pp. 358-366.
Daubechies I, Sweldens W (1996). Factoring wavelet transforms into lifting steps. J. Fourier Anal. Appl. 4 (3): 247-269.
Sweldens W (1995). The lifting scheme: a new philosophy in biorthogonal wavelet construction. Proc. SPIE. 2569: 68-78.
Venkatesh S, Srinivasan S, Chen R (1998). An efficient implementation of a progressive image transmission system using successive pruning algorithm on a parallel Architecture, IEEE, 17-20, DEC. pp. 445- 451.
Yin S, Balchen JG (1997). Image compression through a low rate ultrasonic link in subsea Telerobotic applications (J. Mathematical Imaging and vision) ISSN 0924-9907. 7: 41- 43.